Photoelectron Wave Function in Photoionization: Plane Wave or Coulomb Wave?

ARTICLE *in* JOURNAL OF PHYSICAL CHEMISTRY LETTERS · OCTOBER 2015

Impact Factor: 7.46 · DOI: 10.1021/acs.jpclett.5b01891

6 AUTHORS, INCLUDING:

Samer Gozem

University of Southern California

23 PUBLICATIONS **225** CITATIONS

SEE PROFILE

David Osborn

Sandia National Laboratories

127 PUBLICATIONS **2,354** CITATIONS

SEE PROFILE

John F Stanton

University of Texas at El Paso

251 PUBLICATIONS **10,482** CITATIONS

SEE PROFILE

Anna I Krylov

University of Southern California

179 PUBLICATIONS **7,033** CITATIONS

SEE PROFILE

THE JOURNAL OF PHYSICAL CHEMISTRY Letters

Letter

pubs.acs.org/JPCL

Photoelectron Wave Function in Photoionization: Plane Wave or Coulomb Wave?

Samer Gozem,[†] Anastasia O. Gunina,[†] Takatoshi Ichino,[‡] David L. Osborn,[§] John F. Stanton,[‡] and Anna I. Krylov*[,†]

[†]Department of Chemistry, University of Southern California, Los Angeles, California 90089-0482, United States

[‡]Institute for Theoretical Chemistry, Department of Chemistry, The University of Texas at Austin, Austin, Texas 78712, United States

[§]Combustion Research Facility, Sandia National Laboratories, Livermore, California 94551, United States

Supporting Information

ABSTRACT: The calculation of absolute total cross sections requires accurate wave functions of the photoelectron and of the initial and final states of the system. The essential information contained in the latter two can be condensed into a Dyson orbital. We employ correlated Dyson orbitals and test approximate treatments of the photoelectron wave function, that is, plane and Coulomb waves, by comparing computed and experimental photoionization and photodetachment spectra. We find that in anions, a plane wave treatment of the photoelectron provides a good description of photodetachment spectra. For photoionization of neutral atoms or molecules with one heavy atom, the photoelectron wave function must be treated as a Coulomb wave to account for the interaction of the photoelectron with the +1 charge of the ionized core. For larger molecules, the best agreement with experiment is often achieved by using a Coulomb wave with a partial (effective) charge smaller than unity. This likely derives from the fact that the effective charge at the centroid of the Dyson orbital, which serves as the origin of the spherical wave expansion, is smaller than the total charge of a polyatomic cation. The results suggest that accurate molecular photoionization cross sections can be computed with a modified central potential model that accounts for the nonspherical charge distribution of the core by adjusting the charge in the center of the expansion.

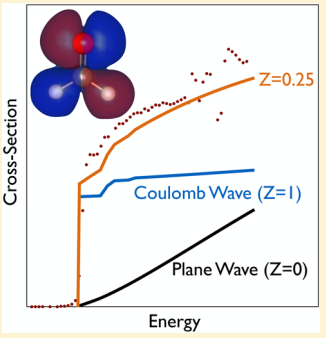

Photoionization and photodetachment experiments are broadly used in chemical physics.[1−3] Photoionization is often used as a tool to identify transient reaction intermediates, whereas photodetachment can be employed to create molecules that are reactive intermediates or otherwise unstable in order to study their properties and spectroscopic signatures.[4−6] Such experiments provide detailed information about the energy levels of the target systems and, often equally important, about the underlying wave functions. However, the interpretation of the photoionization and photodetachment measurements is in many cases not straightforward and requires input from theory. For example, calculations of Franck−Condon factors (FCFs) allow one to connect the features in photoelectron kinetic energy distributions with specific structural changes induced by electron ejection. Particularly challenging is extracting information about the wave functions from the measured cross sections and photoelectron angular distributions.

The information about electronic states of the system is encoded in the so-called photoelectron matrix element, D_k^{IF}:

$$D_k^{\mathrm{IF}} = \mathbf{u}\langle \phi_{\mathrm{IF}}^{\mathrm{d}} | \mathbf{r} | \Psi_k^{\mathrm{el}} \rangle \tag{1}$$

where $\mathbf{r}$ is the dipole moment operator, $\mathbf{u}$ a unit vector in the direction of the polarization of light, and Ψ_k^{el} the wave function of the ejected electron. $\phi_{\mathrm{IF}}^{\mathrm{d}}$ is a Dyson orbital connecting the initial N-electron and the final $N-1$-electron states (I and F, respectively):[7−10]

$$\phi_{\mathrm{IF}}^{\mathrm{d}}(1) = \sqrt{N} \int \Psi_{\mathrm{I}}^{N}(1, ..., n)\Psi_{\mathrm{F}}^{N-1}(2, ..., n)d2 ... dn \tag{2}$$

Equations 1 and 2 are derived within the dipole approximation and assuming strong orthogonality between Ψ_k^{el} and $\phi_{\mathrm{IF}}^{\mathrm{d}}$ and Ψ_{F}^{N-1}. D_k^{IF} enters the expression of the total cross section:[11,12]

$$\sigma_k = \frac{4\pi^2 kE}{c} |D_k^{\mathrm{IF}}|^2 \tag{3}$$

Atomic units are used throughout this letter unless otherwise noted. E is the energy of the ionizing radiation, c the speed of light, and k the magnitude of the photoelectron wave vector related to its kinetic energy, E_k, by $k = \sqrt{2E_k}$. If several channels are open (i.e., when various final Ψ_{F}^{N-1} states are accessible at given energy), the total cross section is simply the sum of the cross sections computed for each channel using its respective Dyson orbital, $\phi_{\mathrm{IF}}^{\mathrm{d}}$.

The calculation of the photoelectron matrix element in eq 1 requires the Dyson orbital and the photoelectron wave function. The Dyson orbital, which is a correlated analogue

Received: August 28, 2015
Accepted: October 28, 2015

DOI: 10.1021/acs.jpclett.5b01891
J. Phys. Chem. Lett. 2015, 6, 4532−4540

of a Hartree−Fock orbital describing the initial state of the ionized electron within Koopmans' theorem, contains all the information about molecular wave functions needed for computing the photoelectron matrix element.[8−10] Dyson orbitals[10] can be computed within the equation-of-motion coupled-cluster (EOM-CC) framework,[13−15] which provides accurate wave functions for closed-shell and various types of open-shell systems. EOM-CC Dyson orbitals include electron correlation and orbital relaxation effects that are neglected in Koopmans' approximation. In this letter, we consider photoejection from closed-shell systems, a situation which usually can be accurately described by the EOM-CC variant known as EOM-IP-CC (EOM-CC for ionization potentials).[16−18] We employ EOM-IP-CC with single and double substitutions (EOM-IP-CCSD).

By using accurate correlated Dyson orbitals, we can focus our attention on approximate treatments of the photoelectron wave function, Ψ_k^{el}. In particular, we test the ability of the simplest possible approximations, i.e., using plane or Coulomb waves, to reproduce experimental cross sections. Our goal is to determine whether eq 1 obtained within the strong orthogonality assumption and the simplest ansatz, a single-center expansion of Ψ^{el}, can capture the correct physics of the problem.

Han and Yarkony pointed out that the strong orthogonality assumption might be too extreme.[19] While various theories of molecular photoionization are capable of providing a quantitatively accurate description of experimental data,[20] applications are often limited by the level of electron correlation that can be employed.[21−24] Alternatively, the Stieltjes imaging approach[25,26] allows one to compute cross sections for photoionization and photodetachment with, in principle, any excited-state electronic structure method by performing a series of necessarily expensive calculations using very diffuse basis sets. In Stieltjes calculations, the state of the ejected electron is approximated by the discretized representation of the continuum states. Because the target state of the system is described by the same many-electron method as the initial state, the strong orthogonality condition is not invoked and the Coulomb and exchange−correlation interactions are described without the assumption of orthogonality. The application of the Stieltjes method with linear response CCSD (a formalism in which the target state energies are identical to EOM-CCSD but transition properties are computed in a different fashion) was shown to yield accurate cross sections for photodetachment[27] and photoionization;[28] however, numerical difficulties can be encountered in the effort to obtain converged results with this procedure. Averbukh and co-workers reported[29] good results for photoionization cross sections of closed-shell molecules obtained using the Stieltjes method with the method known as algebraic diagrammatic construction (ADC).[30] They observed that the accuracy of the calculations deteriorates at higher energies, which they attribute to using Gaussian bases for representing the continuum. By introducing mixed bases in the Stieltjes scheme, i.e., Gaussian and B-splines, they were able to achieve uniform performance over a large energy range.[31] These studies[27−29,31] illustrate that correlated methods such as CCSD and ADC are capable of providing wave functions that are sufficiently accurate for obtaining cross sections within the Stieltjes scheme. Thus, it is desirable to understand the limits of applicability of a simpler model of photoionization (strong orthogonality and single-center expansion) employing Dyson orbitals computed using high-level electronic structure methods. We note that the success of the Cooper−Zare model[32] and its extension to molecular systems[12,33] in fitting and explaining experimental trends in photoionization cross sections and angular distributions[2,34,35] suggests that the underlying assumptions do capture the essential physics of the problem. Similar single-center models have been successfully used in the context of photoionization.[36−39] Han and Yarkony have developed a theoretical framework for determining the state of the ejected electron using the Lippmann−Schwinger equation accounting for nonorthogonality and exchange interactions with the core.[19,40−42] Once the implementation of this much more rigorous framework becomes available, it will become possible to validate approximate treatments such as those explored in this work against their results. However, in the meantime, we are restricted to calibrating our model against experiment, a strategy which we adopt in this letter.

If interactions with the remaining core are completely neglected, the photoelectron can be treated as a plane wave (PW):

$$\Psi_k^{el} = \frac{1}{(2\pi)^{3/2}} e^{i\mathbf{k}\cdot\mathbf{r}} \tag{4}$$

The $(2\pi)^{-3/2}$ factor is the so-called continuum normalization typically used for PWs.[43]

It is convenient to express the PW as a sum of spherical partial waves:[44]

$$e^{i\mathbf{k}\cdot\mathbf{r}} = 4\pi \sum_{l=0}^{\infty} \sum_{m=-l}^{l} i^l R_l(kr) Y_{lm}^*(\hat{r}) Y_{lm}(\hat{k}) \tag{5}$$

where $\hat{r}$ and $\hat{k}$ are the position vector and wave vector, respectively. Each spherical wave is characterized by its energy $E_k = \frac{k^2}{2}$ and angular momentum parameters l and m, and is a product of radial and angular momentum functions. The angular function corresponds to spherical harmonics (Y_{lm}), whereas the radial functions for a PW are expressed using spherical Bessel functions, $R_l(kr) = j_l(kr)$. The expansion origin is placed at the centroid of the Dyson orbital, which is equivalent to orthogonalizing Ψ^{el} to the Dyson orbital.[33] In other words, the origin of the expansion in our approach is fixed such that the strong orthogonality condition is partially satisfied (i.e., Ψ^{el} is orthogonal to ϕ^d). Note that for spherically symmetric species, in which single-center expansion is exact, the centroid of the Dyson orbital always coincides with the origin of the expansion.

The PW approximation assumes no electrostatic or exchange−correlation interactions between the ejected photoelectron and the remaining core, which can be justified by a very large size of the free electron relative to the core. This is certainly a reasonable assumption in the case of photodetachment from anions, where the remaining core is neutral. However, in photoionization of neutral species, the core is positively charged, creating a long-range Coulomb potential that can meaningfully perturb the ejected electron. It is possible to account for these electrostatic interactions by using a Coulomb-distorted plane wave, also known as a Coulomb wave (CW). For a CW, the ionized core is treated as a point charge (i.e., which generates a spherically symmetric field), therefore affecting only the radial part of the photoelectron wave function without affecting the angular part. The CW can also be expanded as a sum of Coulomb partial waves using the same expression as eq 5; however, instead of using spherical Bessel

DOI: 10.1021/acs.jpclett.5b01891
J. Phys. Chem. Lett. 2015, 6, 4532−4540

functions, the radial part is described using a Coulomb radial wave function:[45]

$$R_l(kr, \eta) = (2kr)^l e^{-\pi\eta/2} \frac{|\Gamma(l+1+i\eta)|}{\Gamma(2l+2)} e^{-ikr} \times {}_1F_1(l+1-i\eta, 2l+2, 2ikr) \quad (6)$$

where Γ is the Gamma function and ${}_1F_1$ is the confluent hypergeometric function of the first kind. η is the Sommerfeld parameter, which is equal to $-Z/k$ in atomic units (taking the electron charge to be -1), where Z is the charge of the ionized core and k is the magnitude of the photoelectron wave vector. When $Z = 0$, the CW becomes a PW because the Coulomb radial function becomes a spherical Bessel function. Figure 1

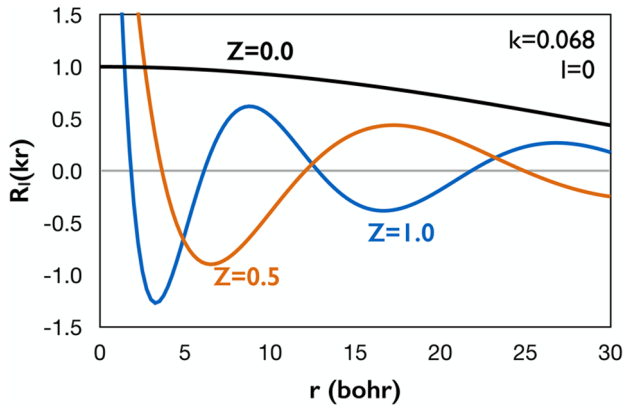

Figure 1. Coulomb radial function for $l = 0$ and $k = 0.068$ au (E_k = 0.0625 eV), with $Z = 0$, 0.5, and 1.0 (black, orange, and blue curves, respectively). The Coulomb radial function with $Z = 0$ is identical to the spherical Bessel function. In the systems studied here, Dyson orbitals do not extend beyond 12 bohr.

shows the radial function, eq 6, for three different values of Z: 0, 0.5, and 1.0. For the same kinetic energy, the CW is more compact along r and displays more oscillations than its PW counterpart. A more detailed comparison between CWs and PWs is presented in Figure S1. Even for small kinetic energies, CWs rise quickly at the origin for small nonzero l, whereas PWs are much slower to rise. For $l = 0$, the PW has a value of 1 at the origin, whereas CWs have a larger value (which is determined by the respective normalization constant) that becomes yet larger as k becomes smaller. This is because slow electrons have a larger probability to be close to the positive charge.

Here we consider several atomic and molecular systems for which reliable experimental cross sections are available. We focus on systems with relatively small ionization-induced structural changes, such that FCFs can be reliably calculated using the double-harmonic Franck−Condon approximation, which allows us to focus on the electronic part of the problem, eq 1. We also do not consider systems that show evidence of ionization via autoionizing resonances; these cases can, in principle, be approached by the extension of EOM-CC theory to metastable electronic states.[46] We are particularly interested in the cross sections near threshold (the origin of the ionization and photodetachment and a few electron volts above it) as this is a key "fingerprint" region that, for example, plays an important role in identifying isomers in reactive mixtures.[47−49]

For all molecules studied in this work, structures are optimized using density functional theory (DFT) with the

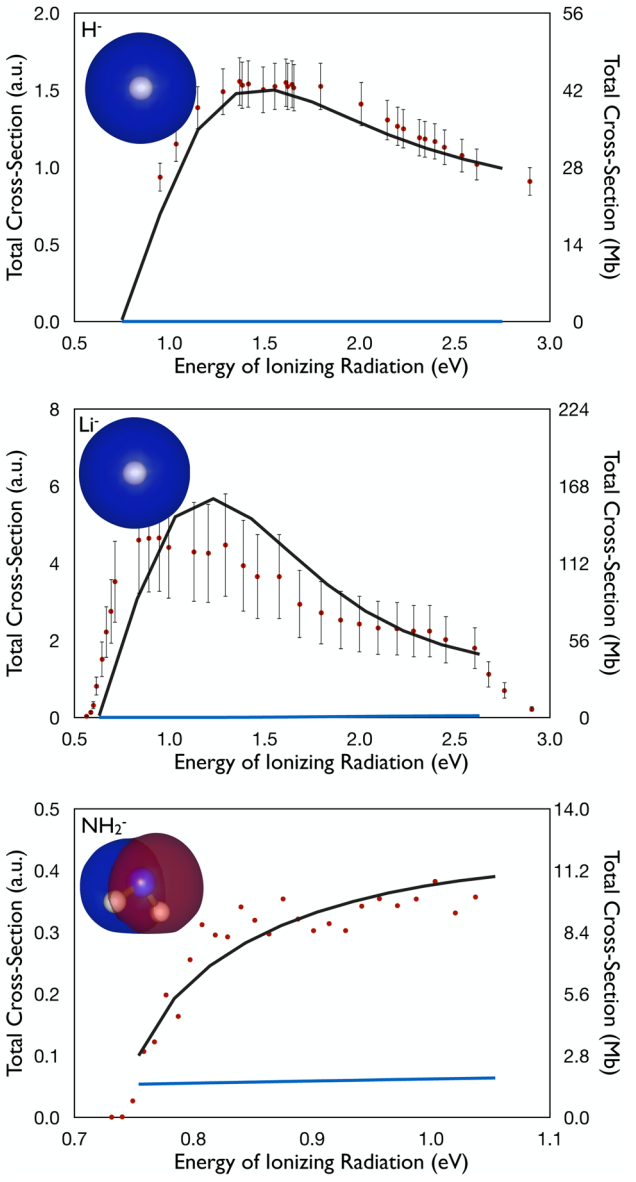

Figure 2. Absolute cross sections for photodetachment from H^-, Li^-, and NH_2^-. Red dots are the experimental values from refs 55 (H^-), 54 (Li^-), and 56 (NH_2^-). Black and blue curves denote cross sections computed using PWs and CWs (with $Z = 1$), respectively. For NH_2^-, only the relative cross sections were measured experimentally; therefore, they have been scaled to match absolute cross sections obtained by calculations. FCFs are included for NH_2^-. The corresponding Dyson orbitals are shown in the top left corners.

ωB97X-D functional.[50] Dyson orbitals are computed in Q-Chem,[51] with the initial and final wave functions, Ψ_I^N and Ψ_F^{N-1}, described by CCSD and EOM-IP-CCSD, respectively. All optimizations and FCF calculations employ the aug-cc-pVTZ basis set. Dyson orbitals for neutral systems are also computed with aug-cc-pVTZ, unless indicated otherwise. Dyson orbitals for the anions are computed with the d-aug-cc-pVQZ basis set (additional augmentation has little to no effect for neutral systems). Cross sections are computed with *ezDyson*[33,52] using experimentally determined ionization energies. FCFs are computed by *ezSpectrum*[53] using DFT (ωB97X-D) structures and frequencies. The details about averaging over molecular orientations, accounting for electronic degeneracies of the

DOI: 10.1021/acs.jpclett.5b01891
J. Phys. Chem. Lett. 2015, 6, 4532−4540

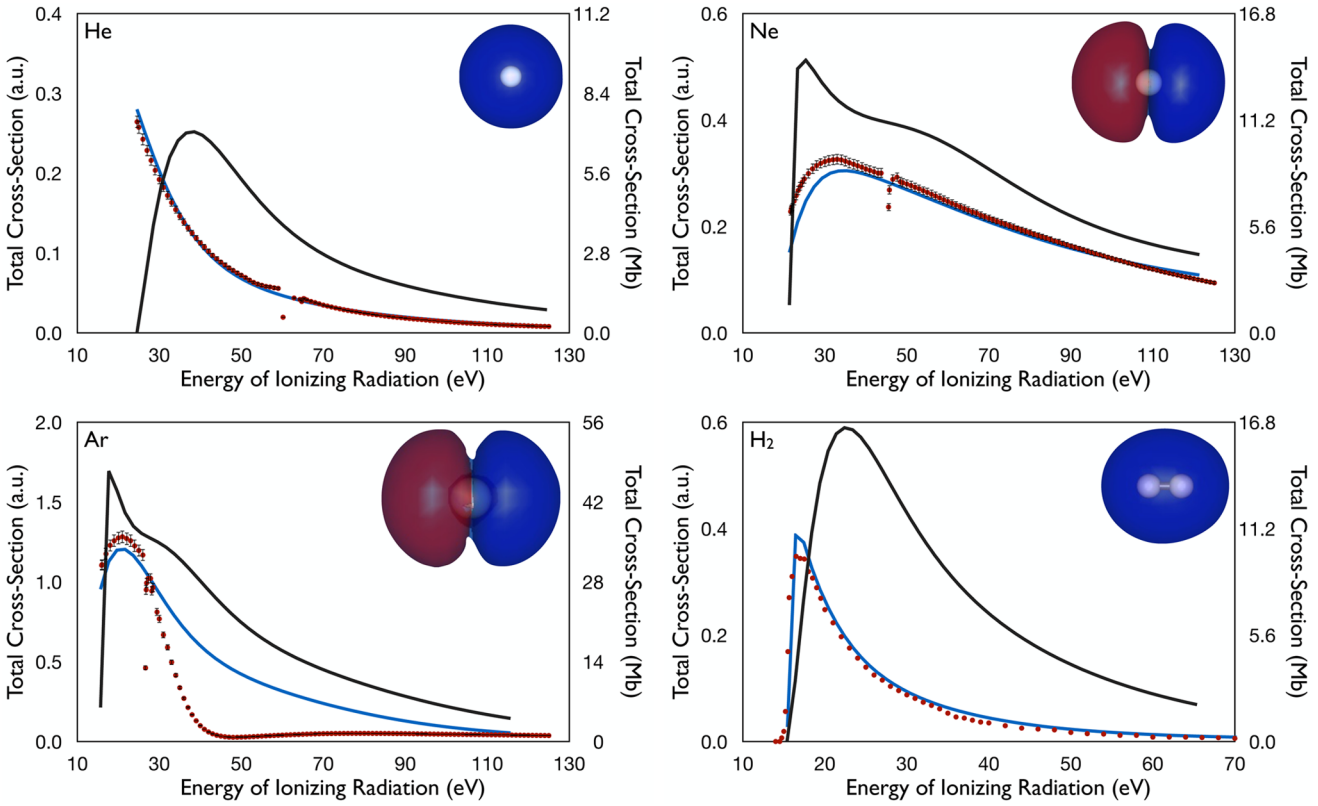

Figure 3. Absolute cross sections for photoionization from He, Ne, Ar, and H_2. Red dots are experimental cross sections.[58,61] Black and blue curves denote cross sections computed using PWs and CWs, respectively. FCFs are included for H_2. For neon and argon, the aug-cc-pV6Z basis set was employed. The corresponding Dyson orbitals are shown in the top right corners.

initial and target states, and incorporating FCFs into the cross-section calculations can be found in the *ezDyson* manual.[52]

The performance of the PW description with EOM-CCSD Dyson orbitals in calculations of the cross sections for photodetachment from small atomic and molecular anions has been tested before.[33] As illustrated in Figure 2, the difference between those computed with PW and CW is huge. As one can see, the PW approach can reproduce the experimental cross sections well; the discrepancies between the computed and measured cross sections are within the experimental uncertainties.[54,55]

However, the same protocol applied for computing photoionization cross sections for small neutral systems (such as He, Ne, Ar, H_2) leads to disastrous results. On the other hand, as illustrated in Figure 3, the calculations using the CW representation (with $Z = +1$) yield very good agreement with the experiments, both in terms of the magnitude and the shape (with the exception of the Cooper minimum in Ar[57] discussed below). The theoretical curves are practically on top of the experimental ones for He, Ne, and H_2. Likewise, the absolute partial cross sections for the three different ionized states of water (Figure 4) show much better agreement with experiment when computed using CWs. We emphasize that both partial cross sections corresponding to three different valence ionized states and the total cross section are reproduced well. We note that our calculations fail to reproduce the Cooper minimum in Ar,[57] a spectral feature at around 47 eV observed in the photoionization spectrum as well as in high-harmonic spectra.[58−60] The Cooper minimum arises because of the node in the Dyson orbital that leads to the change of the sign in the photoelectron matrix element as the outgoing d-wave moves in at higher E_k. Thus, the position of the Cooper minimum is defined by the shape of the Dyson orbital and by Ψ_{el}. The calculations by Wörner et al.[60] failed to reproduce the Cooper minimum when using plane or Coulomb waves and an uncorrelated Dyson orbital. However, they were able to describe the minimum with free electron wave functions computed using effective central potential accounting for exchange interactions with the core. In the Stieltjes imaging calculations,[31] the position of the Cooper minimum was found to be very sensitive to the details of calculations (quantitative agreement with the experiment was achieved only when using a B-spline instead of Gaussian basis, which provides a better description of the continuum).

The better performance of CWs for photoionization of atomic neutral species is not surprising, and one may expect that CWs might also work well for larger neutral targets. However, as illustrated below, the performance is not uniform; in polyatomic systems a better agreement with experiment is sometimes observed for PWs. An optimal description of the photoelectron is often obtained with a CW parametrized with a partial charge, $Z \in [0, 1]$.

We begin with formaldehyde, for which accurate experimental results are available.[63] The results are shown in Figure 5. The CW gives a step-function-like shape, whereas the calculation based on PWs results in a gradually rising curve, which can be rationalized by the more oscillatory behavior of the CWs (Figure 1 and Figure S1). The experimental cross section exhibits features seen in both PW and CW ($Z = 1$) calculations; the sharp rise of the cross section at the ionization threshold is a feature of the CW, whereas the continuing gradual rise with increasing energy is a feature of the PW.

DOI: 10.1021/acs.jpclett.5b01891
J. Phys. Chem. Lett. 2015, 6, 4532−4540

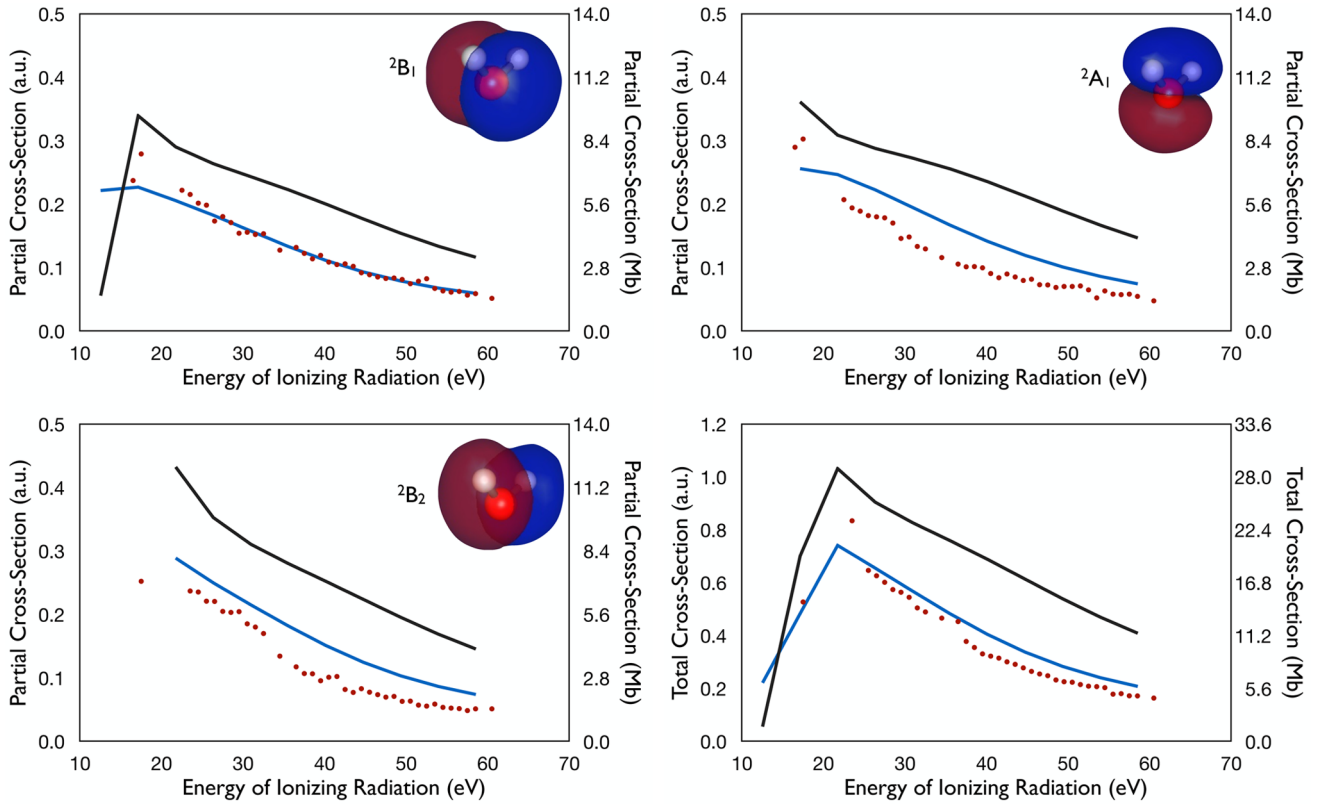

Figure 4. Absolute partial cross sections for the three lowest ionized states of water and the total absolute cross section (excluding contributions from the core-ionized state). Red dots are the experimental cross sections.[62] Black and blue curves denote the cross sections computed using PWs and CWs, respectively. FCFs are not included. The Dyson orbital for each state is shown in the top right corner.

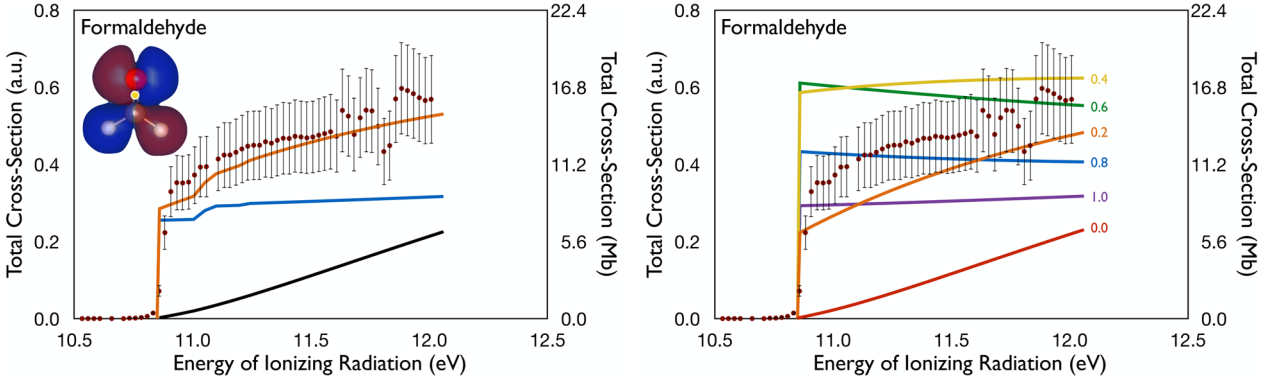

Figure 5. Left panel: Absolute cross sections for formaldehyde photoionization. The experimental cross sections are shown as red dots.[63] The computed values are shown by black (PW), blue (CW with $Z = +1$), and orange (CW with $Z = +0.25$) curves. All computed curves include FCFs. Right panel: The cross sections (without FCFs) using different values of Z. The Dyson orbital and the center of expansion of the PW or CW (yellow circle) are also shown.

Neither PW nor CW ($Z = 1$) provides a good agreement with the experiment. However, using CW with $Z = 0.25$ leads to an excellent agreement, once FCFs are included, both at threshold and at higher energies. A possible reason for this is that the effective charge in the center of expansion is different from 1, as the hole is delocalized. Figure S2a shows the location of the center of the expansion and partial charges in CH_2O^+; as one can see, the position of the Dyson orbital centroid is significantly offset relative to the carbon atom hosting most of the positive charge.

Figure 5 also shows the photoionization spectra of formaldehyde computed using different values of Z. It is clear that the energy profile and absolute value of the electronic cross section depends strongly on the effective charge. Interestingly, the changes in shape and magnitude of the cross-section profiles are not monotonic as Z changes from 0 to 1, such that spectra computed with CWs with intermediate values of Z do not lie between those computed with $Z = 0$ and $Z = 1$. These changes are driven by the shape of the photoelectron radial function, $R_l(kr)$, and its overlap with $r\phi_{IF}^{d}$. This is illustrated in Figure S5, where we plot $r_x\phi_{IF}^{d}$ along a one-dimensional cut for formaldehyde and $R_l(kr)$ for $l = 1$ as a function of Z (we consider only $l = 1$ because the outgoing electron is predominantly a p-wave in this case).

Figure 6 and Figure S3 show the computed and experimental cross sections of other small organic molecules with relatively

DOI: 10.1021/acs.jpclett.5b01891
J. Phys. Chem. Lett. 2015, 6, 4532−4540

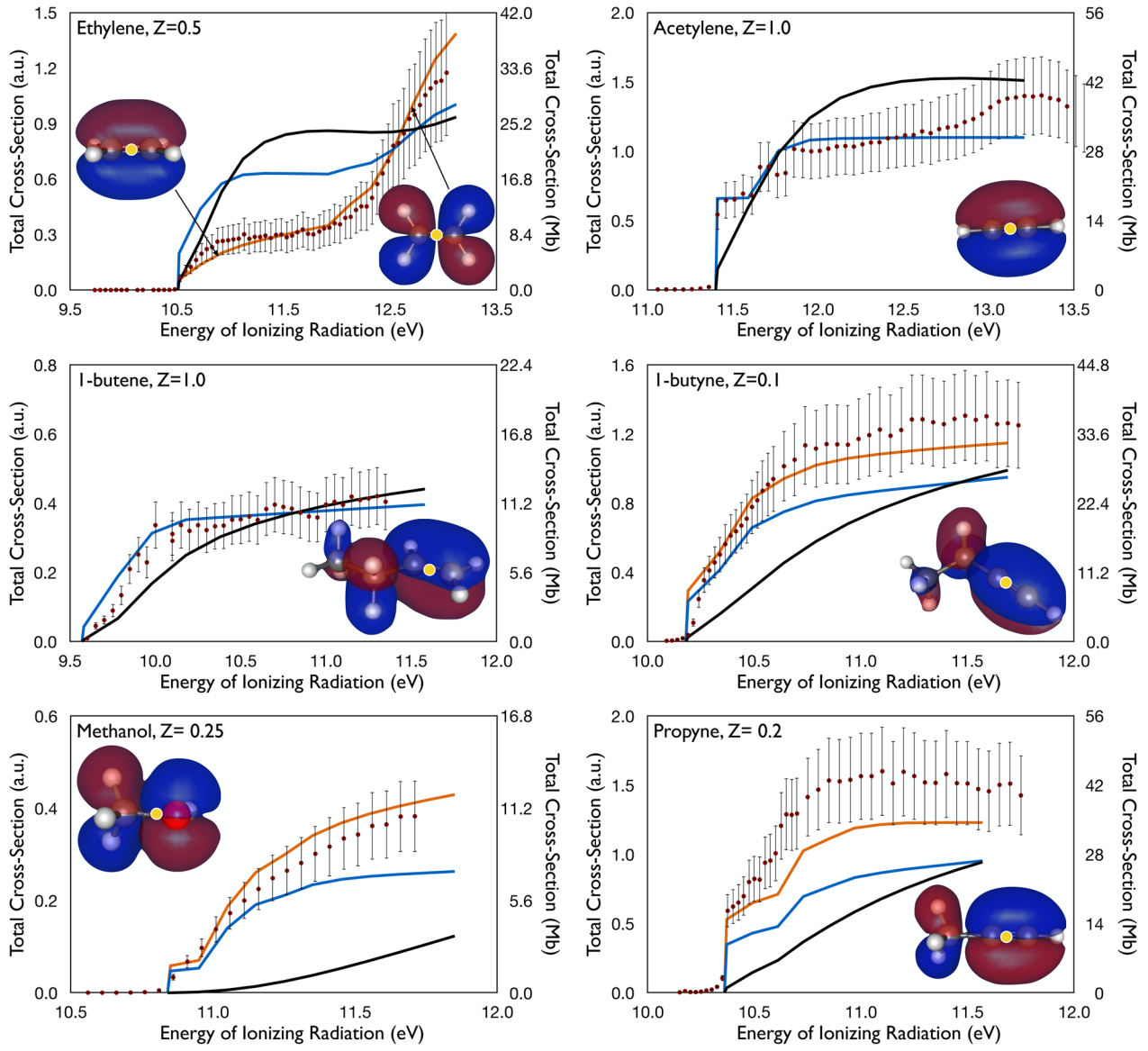

Figure 6. Absolute cross sections for photoionization of ethylene, acetylene, 1-butene, 1-butyne, methanol, and propyne. For ethylene, two ionized states are accessed. The experimental cross sections are shown as red dots. Experimental data are from refs 64 (for acetylene, ethylene, methanol, and propyne) and 65 (for 1-butene and 1-butyne). The computed values are shown using PW (black), CW (blue), and CW with a charge that gives the best fit with experiment (orange, if a good fit is not already obtained with PWs or CWs). All computed curves include FCFs. The Dyson orbitals and the centers of expansion of the PW or CW (yellow circle) are also shown.

short FCF progressions. These molecules are ethylene, acetylene, propene, 1-butene, *cis*-2-butene, 1-butyne, methanol, and propyne. For ethylene and propene, two channels are accessible in the reported energy range. Mulliken charges for the ionized states in these systems are shown in Figure S2 (with hydrogen charges summed onto heavy atoms). While in some cases (e.g., acetylene and 1-butene) good agreement with experiment is obtained using CWs with $Z = 1$, for most systems a better fit is obtained by using CWs with a partial effective charge. In the case of multiple channels (ethylene and propene), the resulting total cross section can be reproduced by using the same effective charge for each channel, which is perhaps fortuitous because we would expect the appropriate choice of partial charge to be dependent on the final state accessed in photoionization. Figure S4 compares the cross-section profiles computed with and without FCFs to elucidate the effect of FCFs. Again, we emphasize good agreement between theory and experiment near the threshold, which can be important for identification of isomers.

To summarize, this work investigated photoionization and photodetachment cross sections in small neutral (He, Ne, Ar, H_2) and anionic (H^-, Li^-, NH_2^-) systems, as well as somewhat larger neutral molecular systems. We find that we can accurately reproduce the experimental spectra for these systems by using the formalism derived within the strong orthogonality assumption using EOM-IP-CCSD Dyson orbitals along with a single-center expansion of the wave function of the photoelectron. However, whereas in the anions the photoelectron wave function can be treated as a PW, in the neutral systems the photoelectron must be treated using CWs (with $Z = 1$) to account for the electrostatic interaction between the photoelectron and remaining core. Our results also illustrate that for photoionization from larger neutral molecules, a relatively simple single-center expansion of the free-electron wave

DOI: 10.1021/acs.jpclett.5b01891
J. Phys. Chem. Lett. 2015, 6, 4532−4540

function appears to provide a reasonable description of the state of the ejected electron, allowing one to compute cross sections that are in good agreement with the experiment. However, the effective charge for the CW that gives the best agreement with the experiment is not always unity. The experimental photoionization spectra often have features that resemble spectra computed both with PWs and with full (Z = 1) CWs. For example, in formaldehyde the cross section rises sharply at the threshold (as in the cross sections computed with the full CW) but then continues to rise gradually after that, as in the PW. This is likely because the photoelectron wave is blind to the charge located far from the expansion center (which is determined by the centroid of the Dyson orbital, in order to partially satisfy the strong orthogonality condition). This is an important result that shows that neither PW nor CW by themselves provides an adequate description of the ejected electron. Also, the generally good agreement of the results suggests that our simple model, which is based on the strong orthogonality assumption, does capture the essential physics even though it neglects the nonspherical symmetry of the electrostatic potential, as well as the correlation and exchange interactions of the ejected electron with the core. Thus, we conclude that accurate photoionization cross sections for molecules can be computed using a modified central potential model that accounts for nonspherical charge distribution of the core by adjusting the charge in the center of the expansion. Contrary to the Stieltjes scheme,[28,29,31] the present approach is significantly cheaper because it does not require calculations with very large basis sets, finding large numbers of approximate eigenstates (e.g., via block Lanczos diagonalization), or solving the moments problem to recover the cumulative oscillator strength for photoionization. This result is of both fundamental and practical importance. On the fundamental side, it shows that the strong orthogonality assumption is justified and that exchange and correlation interactions of the photoelectron with the core have relatively weak effects on the cross section. On the practical side, this finding provides guidance for future theoretical developments. It suggests that this simple ansatz correctly captures underlying physical behavior and can, therefore, be used as a starting point for developing a predictive model for computing photoionization cross sections. What is needed is a procedure for determining the optimal charge Z. We propose variational optimization of this parameter by using numerical solutions of a one-particle Schrödinger equation with a nonspherical Coulomb potential described by the electrostatic potential, $V^{\mathrm{el}}(R, r)$, of the ionized system:

$$\frac{\delta}{\delta Z}\left|\frac{\langle\Psi(Z)|H^{\mathrm{C}}|\Psi(Z)\rangle_L}{\sqrt{\langle\Psi(Z)|\Psi(Z)\rangle_L\langle H^{\mathrm{C}}\Psi(Z)|H^{\mathrm{C}}\Psi(Z)\rangle_L}}\right| = 0 \tag{7}$$

where $H^{\mathrm{C}} \equiv T_k + V^{\mathrm{el}}(R, r)$ and $\Psi(Z)$ is a CW with charge Z, and the integration is done over a finite box of size L. The expression in square brackets in eq 7 is maximized for $\Psi(Z)$ which is the closest approximation to an eigenstate of H^{C}. For example, if V^{el} is just the Coulomb potential created by point charge Z placed in the center of the expansion, the value of the expression in eq 7 equals 1 when $\Psi(Z)$ is a CW with charge Z, because that is the exact solution. The exploratory calculations for formaldehyde using this criterion (see Supporting Information) are encouraging. This full implementation and detailed benchmarks will be pursued in future work.

■ ASSOCIATED CONTENT

Supporting Information

The Supporting Information is available free of charge on the ACS Publications website at DOI: 10.1021/acs.jpclett.5b01891.

Detailed comparison between PW and CW for l = 0−5, Mulliken charges in ionized species, photoionization cross sections for selected molecules with and without FCFs, comparison between photoelectron radial functions with different Z with formaldehyde's Dyson orbital, and exploratory variational optimization of the optimal charge in formaldehyde (PDF)

■ AUTHOR INFORMATION

Notes

The authors declare no competing financial interest.

■ ACKNOWLEDGMENTS

This work is supported by the United States Department of Energy, Basic Energy Sciences through the following grants: DE-FG02-05ER15685 (A.I.K.) and DE-FG02-07ER15884 (J.F.S.). The contribution of D.L.O. is based upon work supported by the U.S. Department of Energy, Office of Science, Office of Basic Energy Sciences. A.I.K. is also a grateful recipient of the Bessel Research Award from the Alexander von Humboldt Foundation. J.F.S. acknowledges additional support from the Robert A. Welch Foundation (Grant F-1283).

■ REFERENCES

(1) Simons, J. In *Photoionization and Photodetachment*; Ng, C. Y., Ed.; Part II of *Advanced Series in Physical Chemistry*; World Scientific Publishing Co.: Singapore, 2000; Vol. *10*.

(2) Sanov, A.; Mabbs, R. Photoelectron imaging of negative ions. *Int. Rev. Phys. Chem.* **2008**, *27*, 53−85.

(3) Reid, K. L. Picosecond time-resolved photoelectron spectroscopy as a means of gaining insight into mechanisms of intramolecular vibrational energy redistribution in excited states. *Int. Rev. Phys. Chem.* **2008**, *27*, 607−628.

(4) Welz, O.; Savee, J. D.; Osborn, D. L.; Vasu, S. S.; Percival, C. J.; Shallcross, D. E.; Taatjes, C. A. Direct kinetic measurements of Criegee intermediate (CH_2OO) formed by reaction of CH_2I with O_2. *Science* **2012**, *335*, 204−207.

(5) Neumark, D. M. Probing the transition state with negative ion photodetachment: experiment and theory. *Phys. Chem. Chem. Phys.* **2005**, *7*, 433.

(6) Neumark, D. M. Probing chemical dynamics with negative ions. *J. Chem. Phys.* **2006**, *125*, 132303.

(7) Linderberg, J.; Öhrn, Y. *Propagators in quantum chemistry*; Academic Press: London, 1973.

(8) Ortiz, J. V. Toward an exact one-electron picture of chemical bonding. *Adv. Quantum Chem.* **1999**, *35*, 33−52.

(9) Hudock, H. R.; Levine, B. G.; Thompson, A. L.; Satzger, H.; Townsend, D.; Gador, N.; Ullrich, S.; Stolow, A.; Martínez, T. J. Ab initio molecular dynamics and time-resolved photoelectron spectroscopy of electronically excited uracil and thymine. *J. Phys. Chem. A* **2007**, *111*, 8500−8598.

(10) Oana, C. M.; Krylov, A. I. Dyson orbitals for ionization from the ground and electronically excited states within equation-of-motion coupled-cluster formalism: Theory, implementation, and examples. *J. Chem. Phys.* **2007**, *127*, 234106.

(11) Bethe, H. A.; Salpeter, E. E. *Quantum mechanics of one and two electron atoms*; Plenum: New York, 1977.

(12) Reed, K. J.; Zimmerman, A. H.; Andersen, H. C.; Brauman, J. I. Cross sections for photodetachment of electrons from negative ions near threshold. *J. Chem. Phys.* **1976**, *64*, 1368−1375.

DOI: 10.1021/acs.jpclett.5b01891
J. Phys. Chem. Lett. 2015, 6, 4532−4540

(13) Krylov, A. I. Equation-of-motion coupled-cluster methods for open-shell and electronically excited species: The hitchhiker's guide to Fock space. *Annu. Rev. Phys. Chem.* **2008**, *59*, 433−462.
(14) Sneskov, K.; Christiansen, O. Excited state coupled cluster methods. *WIREs Comput. Mol. Sci.* **2012**, *2*, 566.
(15) Bartlett, R. J. Coupled-cluster theory and its equation-of-motion extensions. *WIREs Comput. Mol. Sci.* **2012**, *2*, 126−138.
(16) Stanton, J. F.; Gauss, J. Analytic energy derivatives for ionized states described by the equation-of-motion coupled cluster method. *J. Chem. Phys.* **1994**, *101*, 8938−8944.
(17) Stanton, J. F.; Gauss, J. A simple scheme for the direct calculation of ionization potentials with coupled-cluster theory that exploits established excitation energy methods. *J. Chem. Phys.* **1999**, *111*, 8785−8788.
(18) Pieniazek, P. A.; Arnstein, S. A.; Bradforth, S. E.; Krylov, A. I.; Sherrill, C. D. Benchmark full configuration interaction and EOM-IP-CCSD results for prototypical charge transfer systems: Noncovalent ionized dimers. *J. Chem. Phys.* **2007**, *127*, 164110.
(19) Han, S.; Yarkony, D. R. A Lippmann-Schwinger approach for the determination of photoionization and photodetachment cross sections based on a partial wave Green's function expansion and configuration interaction wave functions. *Mol. Phys.* **2012**, *110*, 845−859.
(20) Underwood, J. G.; Reid, K. L. Time-resolved photoelectron angular distributions as a probe of intramolecular dynamics: Connecting the molecular frame and the laboratory frame. *J. Chem. Phys.* **2000**, *113*, 1067−1074.
(21) Fronzoni, G.; Stener, M.; Decleva, P. Valence and core photoionization dynamics of acetylene by TD-DFT continuum approach. *Chem. Phys.* **2004**, *298*, 141−153.
(22) Rohringer, N.; Gordon, A.; Santra, R. Configuration-interaction-based time-dependent orbital approach for ab initiotreatment of electronic dynamics in a strong optical laser field. *Phys. Rev. A: At., Mol., Opt. Phys.* **2006**, *74*, 043420.
(23) Chu, X. Time-dependent density-functional-theory calculation of strong-field ionization rates of H_2. *Phys. Rev. A: At., Mol., Opt. Phys.* **2010**, *82*, 023407.
(24) Natalense, A. P. P.; Lucchese, R. R. Cross section and asymmetry parameter calculation for sulfur 1s photoionization of SF_6. *J. Chem. Phys.* **1999**, *111*, 5344.
(25) Langhoff, P. W. In *Electron Molecule and Photon Molecule Collisions*; Rescigno, T., McKoy, V., Schneider, B., Eds.; Plenum Press: New York, 1979; p 183.
(26) Cacelli, I.; Moccia, R.; Rizzo, A. Gaussian-type-orbital basis sets for the calculation of continuum properties in molecules: The differential photoionization cross section of molecular nitrogen. *Phys. Rev. A: At., Mol., Opt. Phys.* **1998**, *57*, 1895−1905.
(27) Cukras, J.; Decleva, P.; Coriani, S. A coupled-cluster study of photodetachment cross sections of closed-shell anions. *J. Chem. Phys.* **2014**, *141*, 174315.
(28) Cukras, J.; Coriani, S.; Decleva, P.; Christiansen, O.; Norman, P. Photoionization cross section by Stieltjes imaging applied to coupled cluster Lanczos pseudo-spectra. *J. Chem. Phys.* **2013**, *139*, 094103.
(29) Ruberti, M.; Yun, R.; Gokhberg, K.; Kopelke, S.; Cederbaum, L. S.; Tarantelli, F.; Averbukh, V. Total molecular photoionization cross-sections by algebraic diagrammatic construction-Stieltjes-Lanczos method: Benchmark calculations. *J. Chem. Phys.* **2013**, *139*, 144107.
(30) Dreuw, A.; Wormit, M. The algebraic diagrammatic construction scheme for the polarization propagator for the calculation of excited states. *WIREs Comput. Mol. Sci.* **2015**, *5*, 82−95.
(31) Ruberti, M.; Averbukh, V.; Decleva, P. B-spline algebraic diagrammatic construction: Application to photoionization cross-sections and high-order harmonic generation. *J. Chem. Phys.* **2014**, *141*, 164126.
(32) Cooper, J.; Zare, R. N. Angular distribution of photoelectrons. *J. Chem. Phys.* **1968**, *48*, 942−943.
(33) Oana, C. M.; Krylov, A. I. Cross sections and photoelectron angular distributions in photodetachment from negative ions using equation-of-motion coupled-cluster Dyson orbitals. *J. Chem. Phys.* **2009**, *131*, 124114.
(34) Surber, E.; Mabbs, R.; Sanov, A. Probing the electronic structure of small molecular anions by photoelectron imaging. *J. Phys. Chem. A* **2003**, *107*, 8215−8224.
(35) Weichman, M. L.; Kim, J. B.; DeVine, J. A.; Levine, D. S.; Neumark, D. M. Vibrational and electronic structure of the α- and β-naphthyl radicals via slow photoelectron velocity-map imaging. *J. Am. Chem. Soc.* **2015**, *137*, 1420−1423.
(36) Demekhin, P. V.; Ehresmann, A.; Sukhorukov, V. L. Single center method: A computational tool for ionization and electronic excitation studies of molecules. *J. Chem. Phys.* **2011**, *134*, 024113.
(37) Fink, R. F.; Piancastelli, M. N.; Grum-Grzhimailo, A. N.; Ueda, K. Angular distribution of Auger electrons from fixed-in-space and rotating C $1s \rightarrow 2\pi$ photoexcited CO: Theory. *J. Chem. Phys.* **2009**, *130*, 014306.
(38) Siegbahn, H.; Asplund, L.; Kelfve, P. The Auger electron spectrum of water vapour. *Chem. Phys. Lett.* **1975**, *35*, 330−335.
(39) Bishop, D. M. Single-center molecular wave functions. *Adv. Quantum Chem.* **1967**, *3*, 25−59.
(40) Han, S.; Yarkony, D. R. On the determination of intensities for electron photodetachment and photoionization spectra involving states coupled by conical intersections: Total integral cross sections for polyatomic molecules. *J. Chem. Phys.* **2010**, *133*, 194107.
(41) Han, S.; Yarkony, D. R. Determining partial differential cross sections for low-energy electron photodetachment involving conical intersections using the solution of a Lippmann-Schwinger equation constructed with standard electronic structure techniques. *J. Chem. Phys.* **2011**, *134*, 174104.
(42) Han, S.; Yarkony, D. R. On the determination of partial differential cross sections for photodetachment and photoionization processes producing polyatomic molecules with electronic states coupled by conical intersections. *J. Chem. Phys.* **2011**, *134*, 134110.
(43) Gingrich, D. M. *Practical Quantum Electrodynamics*; CRC Press: Boca Raton, FL, 2006.
(44) Sakurai, J. J. *Modern Quantum Mechanics*; Addison-Wesley Publishing Company: Reading, MA, 1995.
(45) Landau, L. D.; Lifshitz, E. M. *Quantum Mechanics: Non-relativistic theory*; Pergamon: Oxford, 1977.
(46) Jagau, T.-C.; Zuev, D.; Bravaya, K. B.; Epifanovsky, E.; Krylov, A. I. A fresh look at resonances and complex absorbing potentials: Density matrix based approach. *J. Phys. Chem. Lett.* **2014**, *5*, 310−315.
(47) Bodi, A.; Hemberger, P.; Osborn, D. L.; Sztaray, B. Mass-resolved isomer-selective chemical analysis with imaging photoelectron photoion coincidence spectroscopy. *J. Phys. Chem. Lett.* **2013**, *4*, 2948−2952.
(48) Lockyear, J. F.; Welz, O.; Savee, J. D.; Goulay, F.; Trevitt, A. J.; Taatjes, C. A.; Osborn, D. L.; Leone, S. R. Isomer specific product detection in the reaction of CH with acrolein. *J. Phys. Chem. A* **2013**, *117*, 11013−11026.
(49) Welz, O.; Zador, J.; Savee, J. D.; Sheps, L.; Osborn, D. L.; Taatjes, C. A. Low-temperature combustion chemistry of n-butanol: Principal oxidation pathways of hydroxybutyl radicals. *J. Phys. Chem. A* **2013**, *117*, 11983−12001.
(50) Chai, J.-D.; Head-Gordon, M. Long-range corrected hybrid density functionals with damped atom-atom dispersion interactions. *Phys. Chem. Chem. Phys.* **2008**, *10*, 6615−6620.
(51) Shao, Y.; Gan, Z.; Epifanovsky, E.; Gilbert, A. T. B.; Wormit, M.; Kussmann, J.; Lange, A. W.; Behn, A.; Deng, J.; Feng, X.; et al. Advances in molecular quantum chemistry contained in the Q-Chem 4 program package. *Mol. Phys.* **2015**, *113*, 184−215.
(52) Gozem, S.; Krylov, A. I. ezDyson User's Manual. http://iopenshell.usc.edu/downloads/ (accessed September 27, 2015).
(53) Mozhayskiy, V. A.; Krylov, A. I. ezSpectrum. http://iopenshell.usc.edu/downloads/ (accessed September 27, 2015).
(54) Kaiser, H. J.; Heinicke, E.; Rackwitz, R.; Feldmann, D. Photodetachment measurements of alkali negative ions. *Eur. Phys. J. A* **1974**, *270*, 259−265.

DOI: 10.1021/acs.jpclett.5b01891
J. Phys. Chem. Lett. 2015, 6, 4532−4540

(55) Smith, S. J.; Burch, D. S. Relative measurement of the photodetachment cross section for H^-. *Phys. Rev.* **1959**, *116*, 1125−1131.
(56) Smyth, K. C.; Brauman, J. I. Photodetachment of electrons from amide and arsenide ions: the electron affinities of NH_2·and AsH_2·. *J. Chem. Phys.* **1972**, *56*, 4620−4625.
(57) Cooper, J. W. Photoionization from outer atomic subshells. A model study. *Phys. Rev.* **1962**, *128*, 681−693.
(58) Samson, J. A. R.; Stolte, W. C. Precision measurements of the total photoionization cross-sections of He, Ne, Ar, Kr, and Xe. *J. Electron Spectrosc. Relat. Phenom.* **2002**, *123*, 265−276.
(59) Farrell, J. P.; Spector, L. S.; McFarland, B. K.; Bucksbaum, P. H.; Gühr, M.; Gaarde, M. B.; Schafer, K. J. Influence of phase matching on the cooper minimum in ar high-order harmonic spectra. *Phys. Rev. A: At., Mol., Opt. Phys.* **2011**, *83*, 023420.
(60) Wörner, H. J.; Niikura, H.; Bertrand, J. B.; Corkum, P. B.; Villeneuve, D. M. Observation of electronic structure minima in high-harmonic generation. *Phys. Rev. Lett.* **2009**, *102*, 103901.
(61) Backx, C.; Wight, G. R.; Van der Wiel, M. J. Van Oscillator strengths (10−70 eV) for absorption, ionization and dissociation in H_2, HD and D_2, obtained by an electron-ion coincidence method. *J. Phys. B: At. Mol. Phys.* **1976**, *9*, 315.
(62) Tan, K. H.; Brion, C. E.; Van der Leeuw, Ph. E.; van der Wiel, M. J. Van Absolute oscillator strengths (10−60 eV) for the photoabsorption, photoionization and fragmentation of H_2O. *Chem. Phys.* **1978**, *29*, 299−309.
(63) Dodson, L. G.; Shen, L.; Savee, J. D.; Eddingsaas, N. C.; Welz, O.; Taatjes, C. A.; Osborn, D. L.; Sander, S. P.; Okumura, M. Vuv photoionization cross sections of HO_2, H_2O_2, and H_2CO. *J. Phys. Chem. A* **2015**, *119*, 1279−1291.
(64) Cool, T. A.; Wang, J.; Nakajima, K.; Taatjes, C. A.; Mcllroy, A. Photoionization cross sections for reaction intermediates in hydrocarbon combustion. *Int. J. Mass Spectrom.* **2005**, *247*, 18−27.
(65) Wang, J.; Yang, B.; Cool, T. A.; Hansen, N.; Kasper, T. Near-threshold absolute photoionization cross-sections of some reaction intermediates in combustion. *Int. J. Mass Spectrom.* **2008**, *269*, 210−220.

DOI: 10.1021/acs.jpclett.5b01891
J. Phys. Chem. Lett. 2015, 6, 4532−4540